Journal of Solid State Chemistry **164,** 131–137 (2002)
doi:10.1006/jssc.2001.9456, available online at http://www.idealibrary.com on IDEAL®

Phenomenology of Polymorphism

IV. The Trimorphism of Ferrocene and the Overall Metastability of Its Triclinic Phase

Siro Toscani,*,[1] Pedro de Oliveira,† and René Céolin*

*Laboratoire de Chimie Physique, Faculté de Pharmacie, Université René Descartes—Paris 5, 4, avenue de l'Observatoire, 75006 Paris, France; and †Laboratoire de Biophysique, Muséum National d'Histoire Naturelle, 43, rue Cuvier, 75005 Paris, France

Received June 5, 2001; in revised form October 31, 2001; accepted November 6, 2001

Structural and thermodynamic data reported in the literature for the three crystalline phases of ferrocene are used to build a topological representation of its (p, T) phase diagram. Two phases (orthorhombic and monoclinic) exhibit stable phase regions whose temperature ranges increase with increasing pressure. The triclinic phase is found to be metastable at any temperature and pressure. In fact, in the (p, T) diagram, it is not associated with any state of lowest energy although it transforms into the monoclinic phase according to a transition which is reversible. This transition occurs in the phase region where the orthorhombic phase is the stable one.

Key Words: **ferrocene; polymorphism; (p, T) diagram; enantiotropy; monotropy; vapor pressure; stability hierarchy; stability domains; phase equilibria.**

1. INTRODUCTION

In a recent article on phase changes in molecular crystals, it was emphasized by Jack D. Dunitz (1) that "from thermodynamics alone one cannot make any detailed statements about the actual structures involved in phase transitions or about the mechanisms involved. … Although the problem of predicting the crystal structure of a compound, given the molecular structure, is still far from being solved, the converse problem can usually be answered: given the crystal structure, show that it is energetically stable, i. e. that it corresponds to an energy minimum … ."

As far as polymorphism is concerned, i.e., different crystal structures for the same component according to the phase rule, it ensues that each crystal structure is energetically stable (even if metastable). The main question to be answered then for industrial and regulatory purposes (2) is that of the stability hierarchy among a set of polymorphs. This was the aim of a series of preceding articles on polymorphism (3–6) in which general rules were proposed (3) for the construction of (p, T) diagrams, and stability hierarchies to be inferred from the vapor pressure criterion according to Ostwald (7). These rules were used to clarify the concept of monotropy (4) and were applied to the trimorphism of sulfanilamide (5) and piracetam (6). In these two cases, the stability inequalities between polymorphs were deduced from the relative location of their sublimation curves in the (p, T) diagram and were compared with those obtained from lattice energy calculations.

In the present article, the case of the trimorphism of ferrocene (bis-(cyclopentadienyl)iron) is presented as another example of construction of a (p, T) diagram resorting to the topological method to locate triple points already applied in the aforementioned articles. Such diagrams, obtained by combining thermodynamic and crystallographic data, allow the stability hierarchy of polymorphs to be inferred from the relative location of the sublimation curves according to the rule "the most stable phase has the lowest vapor pressure." In so doing, absolute vapor pressure values, which are rather tricky to obtain experimentally, are not needed.

The crystal structures of the three solid phases [monoclinic (8, 9), triclinic (10), and orthorhombic (11)] known for ferrocene have been determined. On cooling below 200 K, the monoclinic (M) phase usually transforms into a triclinic (T) phase at 164 K. However, Ogasahara *et al.* (12) have discovered that the molar heat capacity of a low-temperature phase was lower than that measured for the triclinic phase, thus implying the existence of a third phase that was found to be orthorhombic (O). It was obtained either by disintegrating large crystals of monoclinic ferrocene, by cooling them below 164 K followed by annealing for several hours at about 190 K, or by means of low-temperature crystallization experiments (11).

Although the M → T transition turned out to be always reversible, Ogasahara *et al.* concluded that the low-temperature O phase was the thermodynamically stable one below

[1] To whom correspondence should be addressed. Fax: + (33)1-53-73-96-77. E-mail: toscani@pharmacie.univ-paris5.fr.

0022-4596/02 $35.00

242 K, since they observed the O → M transition at this temperature on heating. Consequently, the well-investigated M → T transition at 164 K was thought to occur between metastable phases.

As far as ferrocene is concerned, another aim of this work was to check whether the O phase is the stable one at low temperature according to Ogasahara *et al.* (12), and subsequently to conclude either the existence of a high-pressure stability domain for phase T or its overall metastability.

2. GENERAL RULES FOR THE CONSTRUCTION OF A (*p*, *T*) DIAGRAM

In the case of a trimorphism, 10 triple points are to be determined. By naming S_1, S_2, S_3, *l*, and *v* the solid, liquid, and vapor phases, respectively, these triple points are S_1-*l*-*v*, S_2-*l*-*v*, S_3-*l*-*v*, S_1-S_2-*v*, S_1-S_3-*v*, S_2-S_3-*v*, S_1-S_2-*l*, S_1-S_3-*l*, S_2-S_3-*l*, and S_1-S_2-S_3. They cannot be all stable and hence are located in the phase diagram according to the following rules:

(a) The three (S_i-*l*-*v*) fusion triple points lie on the single *l*-*v* equilibrium curve. By applying Ostwald's rule, according to which, at a given temperature, the stable phase exhibits the lowest vapor pressure, it ensues that the stability degree of the S_i-*l*-*v* triple points increases as temperature does.

(b) At each stable triple point, the extensions of the stable two-phase equilibrium curves are metastable, those of the metastable curves at each metastable triple point are supermetastable, and those of the supermetastable curves at each supermetastable triple point are hypermetastable (3, 13). This is known as the alternation rule which allows the determination of the degree of stability of each triple point with respect to the others.

Since differential scanning calorimetry (DSC) measurements are generally performed on samples in sealed pans or vessels, melting occurs in the presence of a vapor phase that fills the dead volume in the sample container. Thus, melting points correspond to S_i-*l*-*v* triple points. In turn, the S_i-S_j-*v* triple points, whose corresponding solid transitions are not experimentally observed, may be localized by building the phase diagram according to the preceding rules. Furthermore, since melting (S_i-*l*) and solid transition (S_i-S_j) curves may be represented by straight lines up to pressures as high as 200 MPa (3, 4, 6, 13), the dp/dT slopes of these equilibria can be calculated from a set of data obtained at room pressure according to the Clapeyron equation,

$$\frac{dp}{dT} = \frac{\Delta H}{T\Delta V},$$

which incorporates enthalpy and volume variations at the transition temperature. This leads to the location of the solid-solid-liquid (S_i-S_j-*l*) triple points and, in the present case of trimorphism, to that of the S_1-S_2-S_3 triple point, where all S_i-S_j lines converge. These triple points may fall at negative pressure, with no physical significance, as a consequence of the assumed linearity of the S_i-S_j and S_i-*l* equilibrium curves. Indeed, such values are no more than a convenient tool for the topological location of the triple points.

3. THE CONSTRUCTION OF THE (*p*, *T*) PHASE DIAGRAM OF FERROCENE

3.1. The Melting Points of the Three Phases

According to the first rule, the melting triple points O-*l*-*v*, T-*l*-*v*, and M-*l*-*v* have to be situated on the *l*-*v* curve. Only the melting point of phase M has been experimentally determined (14) ($T_{fus} = 448.7$ K and $\Delta_{fus}H = 17.78\ \mathrm{kJ \cdot mol^{-1}}$). The corresponding temperature can be calculated from interception of the *l*-*v* curve (15), Eq. [1], with the sublimation curve (M-*v*) of the M-phase (16), Eq. [2], since the M and *l* phases must have the same vapor pressure at the M-*l*-*v* triple point. By solving the following system,

$$\begin{cases} \ln(p/\mathrm{MPa}) = 8.44 - \dfrac{5602}{(T/\mathrm{K})} & [1] \\ \ln(p/\mathrm{MPa}) = 15.67 - \dfrac{8819}{(T/\mathrm{K})}, & [2] \end{cases}$$

a T_{fus} value of 445.0 K, in very good agreement with the experimental one, is obtained. It is also worth noting that the sublimation enthalpy ($73.3\ \mathrm{kJ \cdot mol^{-1}}$) from Eq. [2] agrees rather well with the more recently determined value of $72.5\ \mathrm{kJ \cdot mol^{-1}}$ (17).

In order to determine the melting points of the O and T phases, their sublimation curves have to be calculated first. Because the sublimation enthalpy of the M phase ($73.3\ \mathrm{kJ \cdot mol^{-1}}$) as well as the transition heats of O → M and T → M transitions (4.145 and $0.854\ \mathrm{kJ \cdot mol^{-1}}$, respectively) are known (18, 19), the sublimation heats of the O and T phases can be estimated by applying the first principle of thermodynamics. The following may be written,

$$\Delta H_{O \to v} = \Delta H_{O \to M} + \Delta H_{M \to v} = 77.4\ \mathrm{kJ \cdot mol^{-1}} \quad [3]$$

and

$$\Delta H_{T \to v} = \Delta H_{T \to M} + \Delta H_{M \to v} = 74.2\ \mathrm{kJ \cdot mol^{-1}}, \quad [4]$$

neglecting the heat capacity differences.

In a Clausius–Clapeyron equation given in the integrated form,

$$\ln p = A - \frac{B}{T},$$

which is the pertinent relation to represent *l*-*v* and S_i-*v* equilibrium curves, constant *B* is directly proportional to the evaporation or to the sublimation enthalpy. Because the *B* value for the M-*v* equilibrium is known, those for the O-*v*

and T-v equilibria may be easily determined: B(O-v) = 9312 and B(T-v) = 8927, from

$$\frac{B}{8819} = \frac{77.4}{73.3} \quad \text{and} \quad \frac{B}{8819} = \frac{74.2}{73.3},$$

respectively.

Constant A values are found by equalizing the vapor pressures of phases O and T to those of the phase M at the O → M and T → M transition temperatures, 242 and 164 K, respectively: A(O-v) = 17.71 and A(T-v) = 16.33, from

$$A - \frac{9312}{(242/\mathrm{K})} = 15.67 - \frac{8819}{(242/\mathrm{K})}$$

and

$$A - \frac{8927}{(164/\mathrm{K})} = 15.67 - \frac{8819}{(164/\mathrm{K})},$$

respectively.

In conclusion, the O-v and T-v sublimation equilibria are represented by Eqs. [5] and [6],

$$\ln(p/\mathrm{MPa}) = 17.71 - \frac{9312}{(T/\mathrm{K})} \qquad [5]$$

$$\ln(p/\mathrm{MPa}) = 16.33 - \frac{8927}{(T/\mathrm{K})}, \qquad [6]$$

respectively.

Consequently, the temperatures of the melting triple points O-l-v and T-l-v are easily calculated by solving the following systems:

$$\begin{cases} \ln(p/\mathrm{MPa}) = 8.44 - \dfrac{5602}{(T/\mathrm{K})} & [2] \\ \ln(p/\mathrm{MPa}) = 17.71 - \dfrac{9312}{(T/\mathrm{K})} & [5] \end{cases}$$

$$\begin{cases} \ln(p/\mathrm{MPa}) = 8.44 - \dfrac{5602}{(T/\mathrm{K})} & [2] \\ \ln(p/\mathrm{MPa}) = 16.33 - \dfrac{8927}{(T/\mathrm{K})}, & [6] \end{cases}$$

which give T(O-l-v) = 400.2 K and T(T-l-v) = 421.4 K, respectively.

From the first rule for constructing phase diagrams, it turns out that M-l-v is the stable melting triple point, since it is situated at the highest temperature, with T-l-v metastable and O-l-v supermetastable.

3.2. The O-T-v Triple Point

The O-T-v triple point is determined by calculating the intersection between the sublimation curves of the O and T phases, i.e., by solving the system of Eqs. [5] and [6], from which T(O-T-v) = 279.0 K.

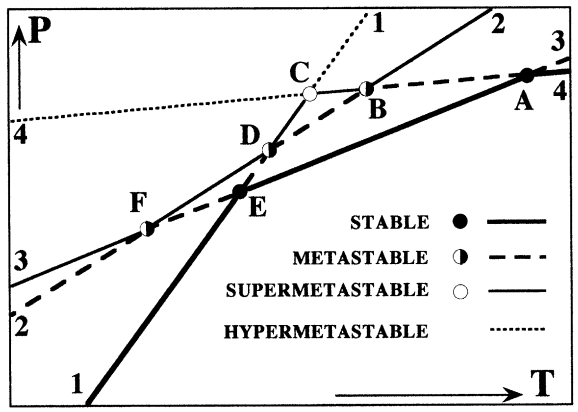

FIG. 1. Topological drawing of the two-phase equilibrium curves involving the vapor phase, with indication of the stability hierarchy. Curves: 1 = O-v, 2 = T-v, 3 = M-v, 4 = l-v. Triple points: A = M-l-v, B = T-l-v, C = O-l-v, D = O-T-v, E = O-M-v, F = M-T-v.

The triple points calculated at this step of construction are shown in Fig. 1 together with the two-phase equilibrium curves involving the vapor phase. It is worth noting that these curves are represented by straight lines according to Oonk (13), notwithstanding the logarithmic form of the related Clausius–Clapeyron equations.

3.3. Preliminary Inferences

The M-l-v, M-O-v, and M-T-v triple points are localized on the M-v equilibrium line in order of decreasing temperature. Since M-l-v is a stable triple point and the M-O-v triple point temperature (242 K) is higher than that of the M-T-v triple point (164 K), it turns out that the M-T-v triple point is metastable by applying the alternation rule. In fact, the M-T-v triple point is situated on the metastable extension of the M-v equilibrium which is stable between the stable M-l-v and M-O-v triple points. In turn, the O-T-v triple point (279 K) delimits the metastable extension of the O-v sublimation equilibrium on increasing the temperature. Because the O-v equilibrium is stable only for $T \leq 242$ K according to the same rule, then triple point O-T-v is expected to be metastable (Fig. 1). In addition, since the T-v and O-v equilibrium curves diverge from the O-T-v triple point on decreasing the temperature, phase T cannot be the stable phase at low temperature. This corroborates the conclusions drawn by Ogasahara *et al.* (12). It is worth noting that all the triple points determined so far possess a common feature: their pressures are very low (values are reported in Table 1).

At this stage, four triple points remain to be located, namely O-T-M, M-T-l, M-O-l, and O-T-l. They may be situated either at high pressure or at very low (or even negative) pressures. As far as phase T is concerned, the goal is to find out whether it is an overall metastable phase (with

TABLE 1
Calculated Coordinates of the 10 Triple Points in the (p, T) Phase Diagram of Ferrocene

Triple point	p/MPa	T/K
M-l-v	1.6×10^{-2}	445.0
T-l-v	7.8×10^{-3}	421.4
O-l-v	3.9×10^{-3}	400.2
O-T-v	1.6×10^{-7}	279.0
O-M-v	1.0×10^{-9}	242.0
T-M-v	2.8×10^{-17}	164.0
O-T-l	($-$ 398.4)	192.4
M-O-l	($-$ 433.9)	174.1
M-T-l	($-$ 471.7)	150.5
O-T-M	($-$ 609.1)	146.6

no stability domain) or a stable one exhibiting a high-pressure enantiotropic behavior.

It also remains to be determined whether the M phase, which is the stable one between 242 and 448.7 K, is a mere low-pressure enantiotropic phase or, conversely, an enantiotropic variety whose stability range is not pressure-limited.

3.4. The O-T-M Triple Point

The position of the O-T-M triple point on the phase diagram lies at the intersection of the O-M and T-M equilibrium lines. Hence, in order for it to be determined, the dp/dT slopes of these equilibria and the corresponding linear equations have to be calculated. These slopes are determined by means of the Clapeyron equation, whose application requires that temperatures and also volume and enthalpy changes at transitions be determined beforehand.

Volume variations have been estimated from crystallographic data reported in the literature. Specific volumes of the M, T, and O phases as linear functions of temperature have been calculated using data measured by Seiler and Dunitz (8) (M and T phases), or derived from the data of Bérar *et al.* (20) (O phase). The equations are the following:

$$[v/(\mathrm{cm^3 \cdot g^{-1}})]\,(\mathrm{M}) = 0.6115 + 1.633 \times 10^{-4}\,[T/\mathrm{K}] \qquad [7]$$

$$[v/(\mathrm{cm^3 \cdot g^{-1}})]\,(\mathrm{T}) = 0.6193 + 1.108 \times 10^{-4}\,[T/\mathrm{K}] \qquad [8]$$

$$[v/(\mathrm{cm^3 \cdot g^{-1}})]\,(\mathrm{O}) = 0.6082 + 1.175 \times 10^{-4} \times [T/\mathrm{K}]. \qquad [9]$$

The endothermal O → M transition occurs at 242 K with an enthalpy variation of 4.145 $\mathrm{kJ \cdot mol^{-1}}$ (22.28 $\mathrm{J \cdot g^{-1}}$). The specific volumes of the O and M phases calculated at 242 K by means of Eqs. [9] and [7], respectively, are 0.6366 and 0.6510 $\mathrm{cm^3 \cdot g^{-1}}$, and hence:

$$\left(\frac{dp}{dT}\right)_{\text{O-M}} = \frac{22.28}{242(0.6510 - 0.6366)}\ \mathrm{J \cdot cm^{-3} \cdot K^{-1}}$$

$$= 6.39\ \mathrm{MPa \cdot K^{-1}}. \qquad [10]$$

Conversely, the endothermal T → M transition occurs at a lower temperature, 164 K, with an enthalpy change of 0.854 $\mathrm{kJ \cdot mol^{-1}}$ (4.59 $\mathrm{J \cdot g^{-1}}$). The specific volumes of the T and M phases calculated at 164 K by means of Eqs. [8] and [7], respectively, are 0.6375 and 0.6383 $\mathrm{cm^3 \cdot g^{-1}}$, giving

$$\left(\frac{dp}{dT}\right)_{\text{T-M}} = \frac{4.59}{164(0.6383 - 0.6375)}\ \mathrm{J \cdot cm^{-3} \cdot K^{-1}}$$

$$= 34.98\ \mathrm{MPa \cdot K^{-1}}. \qquad [11]$$

The linear equations for the O-M and T-M equilibria are then

$$p/\mathrm{MPa} = 6.39\,[(T/\mathrm{K}) - 242.0] \qquad [12]$$

and

$$p/\mathrm{MPa} = 34.98\,[(T/\mathrm{K}) - 164.0], \qquad [13]$$

respectively.

In conclusion, by solving this equation system, the O-T-M triple point coordinates are found to be $p = -609.1$ MPa and $T = 146.6$ K.

At this stage, the linear equation for the O-T equilibrium can be calculated because the corresponding straight line goes through the previously located O-T-v and O-T-M triple points, being then

$$p/\mathrm{MPa} = 4.60\,[(T/\mathrm{K}) - 279.0]. \qquad [14]$$

3.5. The (p, T) Phase Diagram Set-up by the Topological Location of the S_i-S_j-l Triple Points

First, the linear equation of the M-l equilibrium, which exhibits a stable extension at and above ordinary pressure, has to be determined. In order to calculate its dp/dT slope, the volume variation upon melting of phase M as a stable phase at 448.7 K has to be estimated. Data found in the literature (21) on the density of the liquid phase in the temperature range between 453.6 and 627.1 K linearly depend on the temperature according to

$$[\rho/(\mathrm{g \cdot cm^{-3}})] = 1.7674 - 1.2199 \times 10^{-3}\,[T/\mathrm{K}]. \qquad [15]$$

The latter leads to the specific volume value $v_l = 0.8197\ \mathrm{cm^3 \cdot g^{-1}}$ extrapolated at T_{fus}(M), at which $v_{\mathrm{M}} = 0.6848\ \mathrm{cm^3 \cdot g^{-1}}$ according to Eq. [7]. Because $\Delta_{\mathrm{fus}}H$(M) is 17.78 $\mathrm{kJ \cdot mol^{-1}}$ (95.57 $\mathrm{J \cdot g^{-1}}$),

$$\left(\frac{dp}{dT}\right)_{\text{M-}l} = 1.58\ \mathrm{MPa \cdot K^{-1}} \qquad [16]$$

is found by applying the Clapeyron equation. So, the linear equation of the M-l equilibrium is

$$p/\mathrm{MPa} = 1.58\,[(T/\mathrm{K}) - 448.7]. \qquad [17]$$

3.6. The M-T-*l* Triple Point

The M-T-*l* triple point is situated at the intersection of the T-M and M-*l* equilibrium curves, whose linear equations are known. By solving the corresponding system,

$$p/\mathrm{MPa} = 34.98\,[(T/\mathrm{K}) - 164.0] \qquad [13]$$

$$p/\mathrm{MPa} = 1.58\,[(T/\mathrm{K}) - 448.7], \qquad [17]$$

the values arrived at are $p = -471.7$ MPa and $T = 150.5$ K.

3.7. The M-O-*l* Triple Point

The M-O-*l* triple point is located at the intersection of the O-M and M-*l* equilibrium curves. By solving the pertinent system,

$$p/\mathrm{MPa} = 6.39\,[(T/\mathrm{K}) - 242.0] \qquad [12]$$

$$p/\mathrm{MPa} = 1.58\,[(T/\mathrm{K}) - 448.7], \qquad [17]$$

$p = -433.9$ MPa and $T = 174.1$ K are obtained.

At this stage, before constructing the (p, T) diagram, it is worth emphasizing that the open questions concerning the enantiotropic behavior of the M phase and the overall metastability of the T phase can be easily sorted out. Indeed, as M-T-*l* and M-O-*l* triple points are situated at negative pressure, the M-*l* and T-*l* curves, on one hand, and the M-*l* and O-*l* curves, on the other, diverge on increasing the pressure. Consequently, no intersection of the stable M-*l* equilibrium with a metastable extension of either the O-*l* or the T-*l* curves is expected at high pressure: the M phase proves to be the stable one for $T \geq 242$ K and its stability range is not pressure-limited. The same applies to the O phase for $T \leq 242$ K. On the other hand, as the M-T-*v* triple point is located at near-zero pressure and the M-T-*l* and O-T-M triple points are located at negative pressure, the metastable extension of the T-M curve for $p > 0$ cannot intersect any stable equilibrium curve (bearing in mind that no more than three triple points can be located on an equilibrium curve). So, the T phase proves never to be a stable phase on the (p, T) phase diagram, meaning that no stable phase region can be assigned to it.

3.8. The O-T-*l* Triple Point

The O-T-*l* triple point is situated at the intersection of the O-T and T-*l* equilibrium lines. It may be determined via the linear equation of the T-*l* equilibrium which passes through the M-T-*l* and the T-*l*-*v* triple points, leading to

$$p/\mathrm{MPa} = 1.74\,[(T/\mathrm{K}) - 421.4]. \qquad [18]$$

As expected, the slope of the T-*l* equilibrium is steeper than that of the M-*l* equilibrium. By solving the following system,

$$p/\mathrm{MPa} = 4.60\,[(T/\mathrm{K}) - 279.0] \qquad [14]$$

$$p/\mathrm{MPa} = 1.74\,[(T/\mathrm{K}) - 421.4], \qquad [18]$$

the values $p = -398.4$ MPa and $T = 192.4$ K are found for the O-T-*l* triple point.

3.9. Other Inferences

The M-O-*l*, O-T-*l*, and O-*l*-*v* triple points are located on the O-*l* equilibrium line. By taking into account the coordinates of these triple points, the following linear equation is obtained for this equilibrium:

$$p/\mathrm{MPa} = 1.92\,[(T/\mathrm{K}) - 400.2] \qquad [19]$$

As expected, the slope inequalities for the solid–liquid equilibria are

$$\left(\frac{dp}{dT}\right)_{\text{O-}l} > \left(\frac{dp}{dT}\right)_{\text{T-}l} > \left(\frac{dp}{dT}\right)_{\text{M-}l} > 0. \qquad [20]$$

It is worth stating that the high-pressure divergence between the solid–liquid equilibria, derived from the topological location of the S_i-S_j-*l* triple points, is also accounted for by a simple treatment of experimental results concerned with melting at ordinary pressure of the three solid phases of ferrocene.

It was shown above that the melting of the M phase is stable. Conversely, the melting of the T phase, calculated to occur at 421.4 K, is a metastable fusion. The volume variation upon melting has been calculated by taking into account the specific volume of the supercooled metastable liquid ferrocene given by Eq. [15] ($0.7979\ \mathrm{cm^3 \cdot g^{-1}}$) and that of the solid phase obtained from Eq. [8] ($0.6660\ \mathrm{cm^3 \cdot g^{-1}}$). The melting enthalpy may be estimated by applying the first principle of thermodynamics, that is,

$$\Delta H_{\mathrm{T}\to l} = \Delta H_{\mathrm{T}\to\mathrm{M}} + \Delta \mathrm{H}_{\mathrm{M}\to l} = 100.16\ \mathrm{J \cdot g^{-1}}, \qquad [21]$$

neglecting the heat capacity differences.

So, the $(dp/dT)_{\text{T-}l}$ slope is found to be $1.80\ \mathrm{MPa \cdot K^{-1}}$, close to that calculated by the method of the topological location of triple points, steeper than that of the M-*l* equilibrium, and lower than that of the O-*l* equilibrium.

In turn, the melting of the O phase, calculated to occur at 400.2 K, is a supermetastable fusion. The specific volumes of the liquid and solid O phases at equilibrium are $0.7817\ \mathrm{cm^3 \cdot g^{-1}}$ and $0.6552\ \mathrm{cm^3 \cdot g^{-1}}$, respectively. The melting enthalpy is estimated as for the T phase,

$$\Delta H_{\mathrm{O}\to l} = \Delta H_{\mathrm{O}\to\mathrm{M}} + \Delta H_{\mathrm{M}\to l} = 117.85\ \mathrm{J \cdot g^{-1}}, \qquad [22]$$

neglecting the heat capacity differences.

Hence, the $(dp/dT)_{\text{O-}l}$ slope turns out to be $2.33\ \mathrm{MPa \cdot K^{-1}}$. Although this value is 21% higher than

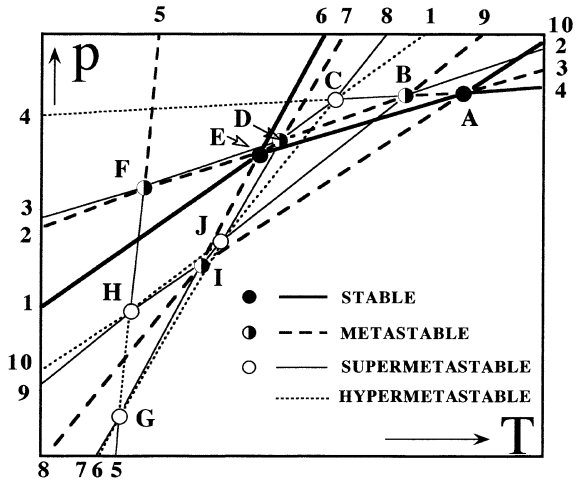

FIG. 2. Topological (p, T) diagram of ferrocene. Two-phase equilibrium curves: $1 \rightarrow 4$ (see Fig. 1), 5 = M-T, 6 = M-O, 7 = O-T, 8 = O-*l*, 9 = T-*l*, 10 = M-*l*. Triple points: A $\rightarrow$ F (see Fig. 1), G = O-T-M, H = M-T-*l*, I = M-O-*l*, J = O-T-*l*.

that arrived at by application of the topological rules, the disclosure of the high-pressure divergence among the solid–liquid equilibrium lines is confirmed.

The complete (p, T) diagram of the ferrocene trimorphism is presented in Fig. 2. In order to give a prominent representation of the domain delimited by the O-M-*v*, the T-M-*v*, and the three fusion triple points, the high-pressure and the negative pressure regions of the graph have been contracted. The latter, which contains the S_i-S_j-S_k and the three S_i-S_j-*l* triple points, is of just a topological interest. The stability domains of the M, O, *l*, and *v* phases are delimited by the stable O-v, M-*v*, O-M, M-*l*, and *l*-*v* equilibrium lines, as shown in Fig. 3. The diagram exhibits two stable triple points, M-O-*v* and M-*l*-*v*, four metastable triple points, T-*l*-*v*, O-T-*v*, M-T-*v*, and M-O-*l*, and four supermetastable triple points, O-*l*-*v*, M-T-*l*, O-T-*l*, and O-T-M. The (p, T) coordinates of the 10 triple points are gathered in Table 1. Among the S_i-S_j-*l* triple points, only M-O-*l* is metastable, as it is the only one to be situated at the intersection of two low-pressure metastable extensions of stable equilibrium lines (O-M and M-*l*); all the others are supermetastable. It can also be noticed that the vapor pressure of the T and M phases at the T $\rightarrow$ M transition temperature, i.e., the M-T-*v* triple point (164 K), is higher than that of the phase O, since the transition between these metastable phases occurs in the stability domain of the third phase (O).

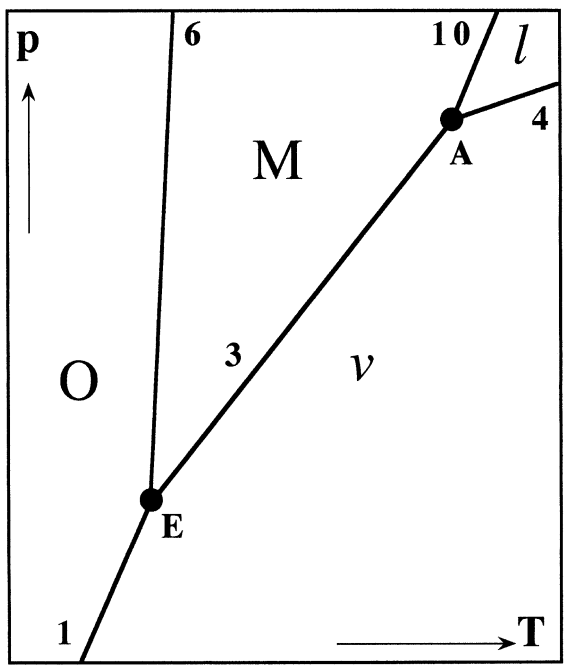

FIG. 3. Topological (p, T) drawing of the stable phase diagram of ferrocene. Stable equilibrium curves: 1 = O-*v*, 3 = M-*v*, 4 = *l*-*v*, 6 = O-M, 10 = M-*l*. Stable triple points: A = M-*l*-*v*, E = O-M-*v*.

4. CONCLUSIONS

Topological rules to locate triple points following a classical approach based upon Ostwald's principle of least vapor pressure have been applied to construct the (p, T) diagram of the ferrocene trimorphism resorting to thermodynamic and crystallographic data reported in literature.

The enantiotropic behavior of the O and M crystal varieties has been ascertained. These phases both possess their own stability range: the O phase is the stable one at low temperature ($T \leq 242$ K) whereas the M phase is the stable form at high temperature. Furthermore, both stability ranges are shown to extend toward even higher pressures as they are not pressure-limited. Conversely, no stable phase region is expected for the T phase in the phase diagram, which shows that the M $\rightarrow$ T transition, at 164 K, occurs in the region where the O phase is stable. It follows that this transition is metastable although it is reversible. This means that Lehmann's definition (22, 23) of monotropy cannot apply to the behavior of the T phase, which can, however, be considered as an example of an overall metastable phase. This outcome fully confirms others from previous experimental works, in particular those by Ogasahara *et al.* (12) based on calorimetric measurements. In addition, as far as trimorphism is concerned, the example of the T phase shows that overall metastability is a necessary but not sufficient item for an overall monotropic behavior to be stated.

In conclusion, such a (p, T) representation may be another example of the heuristic value of the construction method used here because it allows the behavior and the stability degree of each phase under high pressure to be predicted or topologically validated when experimental data are available.

REFERENCES

1. J. D. Dunitz, *Acta Crystallogr. B* **51,** 619–631 (1995).
2. S. Byrn, R. Pfeiffer, M. Ganey, C. Hoiberg, and G. Poochikian, *Pharm. Res.* **12,** 945–954 (1995).
3. R. Céolin, S. Toscani, V. Agafonov, and J. Dugué, *J. Solid State Chem.* **98,** 366–378 (1992).
4. R. Céolin, S. Toscani, and J. Dugué, *J. Solid State Chem.* **102,** 465–479 (1993).
5. S. Toscani, V. A. Dzyabchenko, V. Agafonov, J. Dugué, and R. Céolin, *Pharm. Res.* **13,** 151–154 (1996).
6. R. Céolin, V. Agafonov, D. Loüer, V. A. Dzyabchenko, S. Toscani, and J. M. Cense, *J. Solid State Chem.* **122,** 186–194 (1996).
7. W. Ostwald, *Z. Phys. Chem.* **22,** 289–330 (1897).
8. P. Seiler and J. D. Dunitz, *Acta Crystallogr. B* **35,** 1068–1074 (1979).
9. F. Takusagawa and F. Koetzle, *Acta Crystallogr. B* **35,** 1074–1081 (1979).
10. P. Seiler and J. D. Dunitz, *Acta Crystallogr. B* **35,** 2020–2032 (1979).
11. P. Seiler and J. D. Dunitz, *Acta Crystallogr. B* **38,** 1741–1745 (1982).
12. K. Ogasahara, M. Sorai, and H. Suga, *Chem. Phys. Lett.* **68,** 457–460 (1979).
13. H. A. J. Oonk, "Phase theory," pp. 49–54. Elsevier, Amsterdam, 1981.
14. J. W. Edwards and G. L. Kington, *Trans. Faraday Soc.* **58,** 1334–1340 (1962).
15. F. Scherer, E. O. Fischer, and H. Grubert, *Chem. Ber.* **92,** 2302–2309 (1959).
16. J. W. Hiby and M. Pahl, *Z. Naturforsch.* **7a,** 542–553 (1952).
17. M. A. V. Ribeiro da Silva and M. J. S. Monte, *Thermochim. Acta* **171,** 169 (1990).
18. K. Ogasahara, M. Sorai, and H. Suga, *Mol. Cryst. Liq. Cryst.* **71,** 189–211 (1981).
19. J. W. Edwards, G. L. Kington, and R. Mason, *Trans. Faraday Soc.* **56,** 660–667 (1960).
20. J.-F. Bérar, G. Calvarin, D. Weigel, K. Chhor, and C. Pommier, *J. Chem. Phys.* **73,** 438–441 (1980).
21. L. A. Nisel'son, T. D. Sokolova, and R. K. Nikolaev, *Moscow Univ. Chem. Bull.* **27,** 47–49 (1972).
22. O. Lehmann, "Molekularphysik," Vol. 1, p. 193. Engelmann, Leipzig, 1888.
23. O. Lehmann, "Die Krystallanalyse," pp. 23–27. Engelmann, Leipzig, 1891.